

The Effect of Second-Phase Oxides on the Catalytic Properties of Dispersed Metals: Palladium Supported on 12% WO₃/Al₂O₃

R. ZHANG,^{*,1} J. A. SCHWARZ,^{*,2} A. DATYE,[†] AND J. P. BALTRUS[‡]

^{*}*Department of Chemical Engineering and Materials Science, Syracuse University, Syracuse, New York, 13244; †Department of Chemical and Nuclear Engineering, University of New Mexico, Albuquerque, New Mexico, 87131; and ‡United States Department of Energy, Pittsburgh Energy Technology Center, Pittsburgh, Pennsylvania, 15236*

Received March 13, 1992; revised June 8, 1992

Our earlier study [*J. Catal.* **135**, 200 (1992)] of the properties of dispersed cobalt on a 12% WO₃/Al₂O₃ composite oxide is extended here to palladium. Temperature-programmed reduction (TPRd), transmission electron microscopy (TEM), X-ray photoelectron spectroscopy (XPS), and catalyst performance testing using H₂/CO methanation as a test reaction were used in this study. We find for this system, where surface compounds do not form, that the controlling factor in the performance of Pd/12% WO₃/Al₂O₃ catalysts is the Pd loading in relation to the number of adsorption sites available on the second-phase oxide that can accommodate the Pd precursor. The intrinsic activity of Pd/Al₂O₃ is about one order of magnitude greater than that of Pd/WO₃. The lower activity of the latter appears to be due to Pd–W interactions. © 1992 Academic Press, Inc.

INTRODUCTION

Two major reasons for conducting research on the synthesis of catalytic materials are: (1) to find new or improved catalysts for a particular application, either using modifications of existing materials or new classes of materials; and (2) to establish the relationships between preparative procedures and the structure and properties of the final catalyst. In the latter case, the objective is to understand how the choice of starting materials and synthesis conditions influence catalyst properties. Success here can lead to the identification of general principles and strategies for preparing catalysts with specific properties.

This study is a continuation, in part, of our earlier work using composite oxides as carriers for catalytic metals. We seek in these studies to determine, among other things, the effect of the second-phase oxide

on the catalytic properties of dispersed metals. We have, in our arsenal of synthesis strategies, the concept of selective metal–support exchange or pH-directed adsorption/impregnation. This proposal was originally thought to be limited to exploiting the differences in charge on each oxide surface at a pH spanning the point of zero charge (pzc) of each of the pure oxides comprising the composite. For example, we have recently shown that Co²⁺ ions could be selectively mounted onto the tungsten oxide phase of a 12% WO₃/Al₂O₃ composite oxide (1). Here the catalysts studied were prepared at suitable pH consistent with the selective metal–support exchange hypothesis. While this simple idea has proven to have merit, we find that there are additional degrees of freedom (and obviously constraints) that can be implemented into this catalyst design strategy.

The pzc is related to the equilibria describing the protonation/deprotonation of hydroxyl groups on an oxide surface. It is an index for assessing when ion adsorption, which is controlled by electrostatic interac-

¹ Scientific Committee of Lanzhou, People's Republic of China.

² To whom correspondence should be addressed.

tions, will be favorable. Another parameter, related to the equilibrium constants, provides a measure of the fraction of charged sites when the pH is equal to the pzc (2). At this value, *although the net surface charge is zero*, there exists some inventory of positive, negative, and neutral sites. If the pH is lowered below the pzc, the negative charge density will decrease *but* it is still possible to transfer aqueous cations to these sites. Thus, we find that a greater range of pH values than simply those spanning the pzc of the pure supports can be considered in the design strategy.

In the Co//WO₃/Al₂O₃ study mentioned earlier, a relatively high loading of cobalt was used, 6 wt%. This value was chosen to ensure enough sensitivity for characterization by XPS and also to ensure the reducibility of the cobalt phase for reaction studies, it being well established that low loadings of supported cobalt are difficult to reduce (3). If concentrations of the active catalytic ion are too high, there might not be enough suitable adsorption sites to accommodate all the ions on the desired phase. Indeed, this was what was found. Furthermore, there is the possibility of a complex inventory of surface compounds which could develop simply on the basis that the carrier is a mixed oxide.

The objective of the present study is to identify and better define limitations in the synthesis strategy we have designated as selective metal-support exchange. We use Pd²⁺ cations as the catalytic precursor because they can be easily reduced at low weight loadings (4), it is the primary ion at the low pH used during preparations (5), and under the temperature conditions of characterization and reaction no known surface compounds are formed (6). We use as our support, the 12% WO₃/Al₂O₃ composite, because we have considerable data on the properties of this carrier.

Temperature-programmed reduction (TPRd) data of the dried precursors provides us with signatures for better understanding the partitioning of Pd between WO₃ and Al₂O₃. The calcined catalysts were ex-

amined by transmission electron microscopy (TEM) and the catalysts after reduction were studied using XPS. Finally, the catalytic properties of the composite oxide supported Pd were studied in relation to that metal's properties when supported on each of the pure phases. Steady-state CO hydrogenation was used as the test reaction.

It is useful at this point to provide an additional motivation for our research in this general area. From a practical point of view, there is considerable interest in optimizing the performance of catalyst systems by proper regulation of their preparative procedures. This is particularly true for those systems that offer the possibility for design by the selective metal-support exchange hypothesis. For example, Co//WO₃/Al₂O₃ as well as Ni//WO₃/Al₂O₃, Co//MoO₃/Al₂O₃, and Ni//MoO₃/Al₂O₃ are traditional hydrodesulfurization catalysts (7). Other systems might include Rh//CeO₂/Al₂O₃ extensively studied for its application in automotive pollution control (8) and V₂O₅//TiO₂/SiO₂ the selective reduction catalyst (SCR) for NO_x abatement (9).

EXPERIMENTAL

MATERIALS

The alumina used in this work was derived from ground (40–80 mesh) 1/16" extrudate, γ phase, obtained from American Cyanamid, Lot 85-NA-1402, having a BET surface area of 150 m²/g and pore volume of 0.48 cc/g. It was treated at 875 K for 24 h before use. The tungsten oxide was 99.7% tungsten trioxide from Alfa, Lot B021. Tungsten oxide is nonporous (average particle size \sim 0.04 μ m) with a BET surface area of 1 m²/g. The WO₃ was calcined at 875 K for 24 h before use. The 12% WO₃/Al₂O₃ composite was made by dry impregnation of ammonium metatungstate [(NH₄)₆H₂W₁₂O₄₀ · 5H₂O] obtained from GTE Sylvania. The composite oxide was dried at 380 K overnight and calcined at 875 K for 24 h. Its BET area was 131 m²/g. The point of zero charge of each support was determined by mass titration and the values for Al₂O₃,

TABLE 1A
Catalyst Preparation Conditions for 3% Pd Loading

	Support (g)	Pd(NO ₃) · 6H ₂ O (g)	H ₂ O (ml)	pH	Time (min)	Loading of Pd (%)
Pd/Al ₂ O ₃	1.01	0.37	2.5	1.0	10	3.3%
Pd/WO ₃ /Al ₂ O ₃	1.02	0.29	2.5	0.45	10	3.6%
Pd/WO ₃	1.08	0.65	1	-0.17	10	2.5%

WO₃, and 12% WO₃/Al₂O₃ were 8.5, 4.08, and 6.08 (10). All samples were stored in a dry box purged with N₂. Palladium oxide was made by calcining Pd(NO₃)₂ at 523 K for 2.5 h.

CATALYSTS

The catalysts were prepared from a palladium (II) nitrate precursor (Palladium Metal Basis 41.28%) obtained from Johnson Matthey, lot no. 042182. Since equal weight loadings of Pd on each support were required, the procedures used to prepare catalysts had to be carefully controlled. Thus, preliminary experiments were conducted and based on those results, catalysts for characterization and performance evaluation were prepared. The preliminary experiments were performed at two levels. Equilibrium adsorption experiments using 2 g of each support and 25 cm³ of electrolyte (0.027 mol/liter) were conducted. The initial pH of the precursor solution was 1.6. Following these, dry impregnation and pseudo-wet impregnation methods were employed. The volume of water used for the WO₃ support was scaled to the mass of WO₃ used based on a water/mass ratio that we used in an earlier study (10). The conditions for pseudo-wet impregnation are given in Table 1A. We employ this method in which an amount of solution in excess of the pore volume of the support is used. The rationale is that under these conditions, a more homogeneous deposition of the precursor, approximating the processes occurring during adsorption/impregnation, results. Follow-

ing their preparation, the solids were filtered and then dried at 360 K for 1 h. The weight loadings on the dried catalysts prepared by both methods were determined by extensive washings of palladium from the support with 0.1 N NH₄OH followed by 69.0–71.0% HNO₃ at 373 K and then analysis by AA. The Perkin-Elmer Model 2380 Spectrophotometer was calibrated using Aldrich Chemical Company palladium atomic adsorption standard solution (Lot 04201LW). Replicate runs demonstrated that our reproducibility was ± 0.04 ppm. Additional samples with loadings of ~ 1 and 9% by weight were prepared by the pseudo-wet impregnation method. The conditions are given in Table 1B. Characterization and performance studies were conducted only on those samples prepared by the pseudo-wet impregnation method.

CATALYST CHARACTERIZATION: APPARATUS AND PROCEDURES

TPRd

A complete description of the TPRd unit can be found elsewhere (11). It consists of a gas handling system, thermal conductivity cell and associated electronics (Fisher, Model 1200 gas partitioner), linear temperature programmer (Omega, Model CN-2011J), recorder (IBM PC), sample holder, furnace, and cold traps.

In these experiments, 100 mg of nonactivated and nonpassivated palladium catalyst was dehydrated in a 100 cm³/min argon stream by heating from room temperature

TABLE IB
Catalyst Preparation Conditions for 2, 3.6, and 9% Pd Loading

	Support (g)	Pd(NO ₃) · 6H ₂ O (g)	H ₂ O (ml)	pH	Time (min)	Loading of Pd (%)
Pd/Al ₂ O ₃	1.0	0.09	2.5	1.1	10	1.9%
Pd/WO ₃ /Al ₂ O ₃	1.02	0.29	2.5	0.45	10	3.6%
Pd/WO ₃	1.04	0.64	2.5	-0.04	10	8.9%

to 423 K at a heating rate of 5 K/min. The system was held at 423 K for 1 h and cooled to room temperature. It was further cooled to about 210 K with dry ice. When the system temperature was stable, the carrier gas was switched to an 8.7% H₂ + Ar gas stream with a flow rate of 40 cm³/min and flushed for 15 min. The system was then heated from 210 to 773 K at a heating rate of 20 K/min. During the heating process, the hydrogen signal was monitored continuously. The supports themselves showed no H₂ consumption during blank runs.

TEM

Calcined catalyst samples (875 K for 24 h) were examined in a JEOL 2000 FX TEM at 200 keV. The TEM results we report are for those of the "oxidized" catalyst, not the reduced catalyst, so we are not seeing palladium metal but palladium oxide. The powders were dusted onto holey carbon film supported on copper grids. Elemental analysis was performed using a Tracor Northern energy dispersive spectroscopy system (EDS) equipped with a Be window X-ray detector. Quantitative analysis was performed using the standardless analysis program SMTF.

XPS

The XPS measurements were performed with a Leybold LHS-10 instrument equipped with a DS5 data acquisition system. The instrument has an auxiliary sampling port with an associated microreaction chamber (approx. 30 cm³) that allows sam-

ples to be treated at or above atmospheric pressure. The magnesium anode (MgK α = 1253.6 eV) was operated at 13 kV and 20 mA, and the pass energy of the analyzer was 100 eV. The instrument operates at a vacuum of 2×10^{-9} mbar (2×10^{-7} Pa) or lower. The detection area on the sample was approximately 3×7 mm.

A thin 1-cm diameter precalcined catalyst wafer, formed from the powdered catalysts precalcined at 875 K for 24 h, was sandwiched between tantalum foils and attached to a heatable transfer rod. After insertion of the transfer rod into the reactor zone, a 5-min evacuation of the reactor was performed followed by the reduction treatment. The reduction was performed in a hydrogen flow of 10 cm³/min. The temperature was programmed to ramp with a heating rate of 10 K/min to 473 K and was then held at 473 K for 2 h. The catalyst was then cooled to room temperature in the hydrogen flow. After completion of these treatments, the catalyst was immediately transferred to the XPS analysis position via vacuum interlocks.

The Pd 3d transition was used to identify the palladium species on the catalyst surface. For γ -alumina supported catalysts, the Al 2p line from the alumina support was used as the binding energy reference (74.5 eV) for correction due to sample charging. For samples not containing Al₂O₃, the C 1s peak (284.6 eV) due to hydrocarbon contamination was used as a binding energy reference. The binding energies reported were found to be reproducible to ± 0.2 eV. Peak

areas were calculated using the DS-5 software. The peak areas were used to calculate the average Pd particle sizes according to the model of Kerkhof and Moulijn (12).

CATALYST PERFORMANCE: APPARATUS AND PROCEDURES

TPD Unit

This apparatus is composed of a temperature programmer, mass flow controllers, a tubular reactor, a mass analyzer, and an IBM PC for data retrieval. The reactor temperature was programmed and controlled by a temperature programmer. The product gas is analyzed by the mass analyzer and recorded by the IBM PC. Details of this apparatus are described elsewhere (13). The characterization and performance studies described below were performed in this apparatus.

TPRx

Before TPRx, the dried catalysts were reduced according to the following schedule: 100 mg samples were heated in 50 cm³/min H₂ flow from room temperature to 423 K at a rate of 5 K/min, held there for 1 h, and then heated further to 473 K and reduced in pure H₂ for 2 h. The carrier gas was switched to He at a flow of 30 cm³/min and kept overnight at 373 K to purge the residual H₂ from the catalyst surface. Following cooling to room temperature, a number of CO (0.25 cm³/pulse) pulses was injected to saturate the catalyst surface. The CO gas was preheated and kept at low pressure to prevent the formation of carbonyls (14). After the pulsing sequence, the system was flushed by a 30 cm³/min helium stream for 10 min. The system was heated from room temperature to 873 K in a 30 cm³/min hydrogen stream at a heating rate of 20 K/min. Peaks of $m/e = 2, 15, 28, 30,$ and 44 were monitored during the heating process.

Methanation

These experiments were performed over a temperature range between 475 and 553

K. A H₂/CO = 3/1 gas mixture was used as the reactant at a flow rate of 30 cm³/min. The reduced catalyst was heated to 473 K and the temperature was increased in steps. After each temperature step, the system was held for 10 min to reach a steady reaction rate. Peaks of $m/e = 2, 15, 28, 30,$ and 44 were monitored continuously. The sequence of temperatures was changed in which higher temperatures in the range studied were selected first to ensure that data collected at higher temperatures were not influenced by structural changes that may have occurred at lower reaction temperatures. The Arrhenius plots were reversible, an indication that no such structural modifications occurred. The maximum conversion did not exceed 7% for the most active catalyst. After the reaction sequence described above was performed, the system was flushed with a 30 cm³/min helium stream for 5 min and cooled to room temperature. Blank runs over each support showed no activity over the temperature range 470–600 K.

RESULTS

We begin our presentation of results with a description of the pH-dependent surface charge that develops on WO₃ and Al₂O₃ in aqueous environments. This is an appropriate starting point because it provides the framework which will facilitate the readers' understanding of the partitioning of Pd²⁺ cations between each of the phases of the WO₃/Al₂O₃ support. Figure 1 is a "cartoon" that qualitatively describes the electric charge structure that is possible on the composite oxide. Figure 1 was constructed using data reported elsewhere for Al₂O₃ (15) and our estimate for the pH-dependent surface charge development on WO₃. This latter case is difficult to assess by direct experimental measurement because of the low surface area of unsupported WO₃. The ordinate in Fig. 1 is the fraction of positive, negative, and neutral charge present on the surface of Al₂O₃ and WO₃ over a range of pH. There will be slight modification of these results at

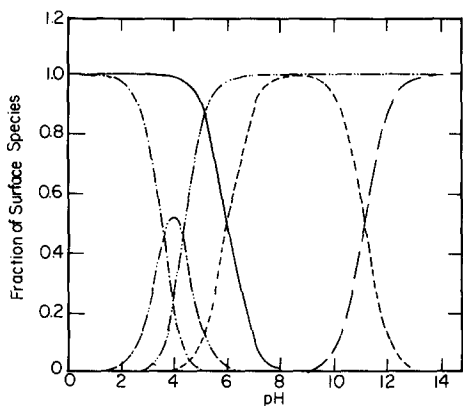


FIG. 1. Schematic of the pH-dependent surface charge development on WO_3 and Al_2O_3 . Symbols: —, $\text{Al}_2\text{O}_3\text{-OH}_2^+$; ---, $\text{Al}_2\text{O}_3\text{-O}^-$; ----, $\text{Al}_2\text{O}_3\text{-OH}$; - · - ·, $\text{WO}_3\text{-OH}_2^+$; - - - -, $\text{WO}_3\text{-O}^-$; - · - · - ·, $\text{WO}_3\text{-OH}$.

different ionic strengths of electrolyte (16). The results show that at pH less than the pH_{pzc} of WO_3 there is a negative charge population on its surface. These can act as receptor sites for Pd^{2+} cations during catalyst preparation. On the other hand, the Al_2O_3 surface contains only positive sites, a template which is not favorable to cation adsorption.

CATALYST PREPARATION

Figure 2 shows the amount of Pd^{2+} adsorbed as a function of time for each of the supports: WO_3 , Al_2O_3 and the composite. Equilibrium is attained in ~ 15 min during which time the pH of the solution continually increased from its initial value of 1.6 for each case. The equilibrium pH was lowest for WO_3 (~ 1.6) and highest for Al_2O_3 (~ 4), indicating that the buffering action of this series decreases in the order $\text{WO}_3 > 12\% \text{WO}_3/\text{Al}_2\text{O}_3 > \text{Al}_2\text{O}_3$ for this background electrolyte.

The results shown in Fig. 2 are reported on a weight basis. They show that the composite adsorbs more Pd^{2+} than either Al_2O_3 or WO_3 . The results of Fig. 2 suggest that the WO_3 phase of the composite could be contributing to an enhancement in adsorption when compared to Al_2O_3 alone. The

weight loading on the composite that corresponds to the plateau is $\sim 1.7\%$, while the concentration of Pd^{2+} in solution was sufficient to mount 3% by weight of metal assuming all the Pd was transferred to the support, demonstrating that the adsorption/exchange component of Pd derived from wet impregnation cannot be neglected. This was unlike what we found for the Co system and made the preparation of catalysts with equal weight loadings on different supports using pseudo-wet impregnation difficult. We resorted to a trial-and-error procedure (see Table 1B), adjusting solution concentrations and measuring resulting loading levels.

TPRd

Figures 3, 4, and 5 show the TPRd profiles for reference compounds and various weight loadings of Pd on selected supports. The reduction spectra for the precursor ($\text{Pd}(\text{NO}_3)_2$) and PdO are presented in Fig. 3. They are characterized by extremely sharp peaks centered at ~ 375 K for the precursor and 280 K for PdO. They will provide the basis for analyzing the TPRd results from the supported catalysts.

Figure 4 shows TPRd profiles for Pd at approximately the same weight loadings ($\sim 3\%$) on (a) Al_2O_3 , (b) 12% $\text{WO}_3/\text{Al}_2\text{O}_3$, and (c) WO_3 . Since the weight loadings are slightly different, it is not possible to quantitatively discuss peak heights at this point. However, the following trends are apparent.

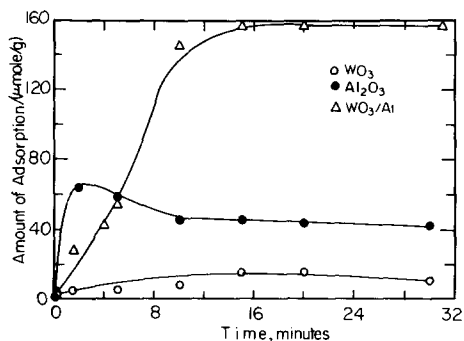


FIG. 2. Adsorption data for uptake of Pd^{2+} on each of the supports.

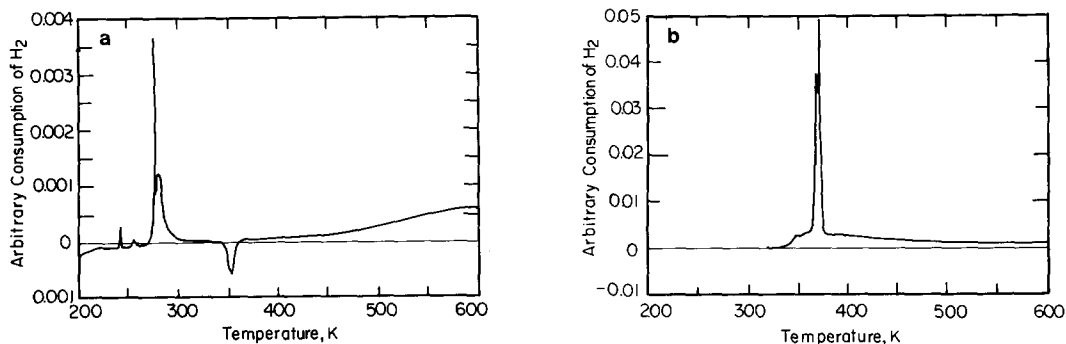


FIG. 3. TPRd profiles for reference compounds: (a) PdO; (b) Pd(NO₃)₂.

Two peaks are found for the Al₂O₃ and composite supported Pd; they have peak maxima that coincide quite well with the reference compounds. The WO₃-supported Pd shows essentially one peak at 280 K (with a complicated but small H₂ consumption occurring for temperatures between 290–400 K). This intense peak coincides with the reference PdO. It appears that either during

the adsorption or mild drying of this material, the Pd precursor is converted entirely into PdO. On the other hand, the Pd precursor that adsorbs on Al₂O₃ is adsorbed both intact and with a portion converted to the oxide. The trends in the peak heights for Pd supported on the composite suggest that on this support more of the precursor is converted to the oxide, perhaps due to the pres-

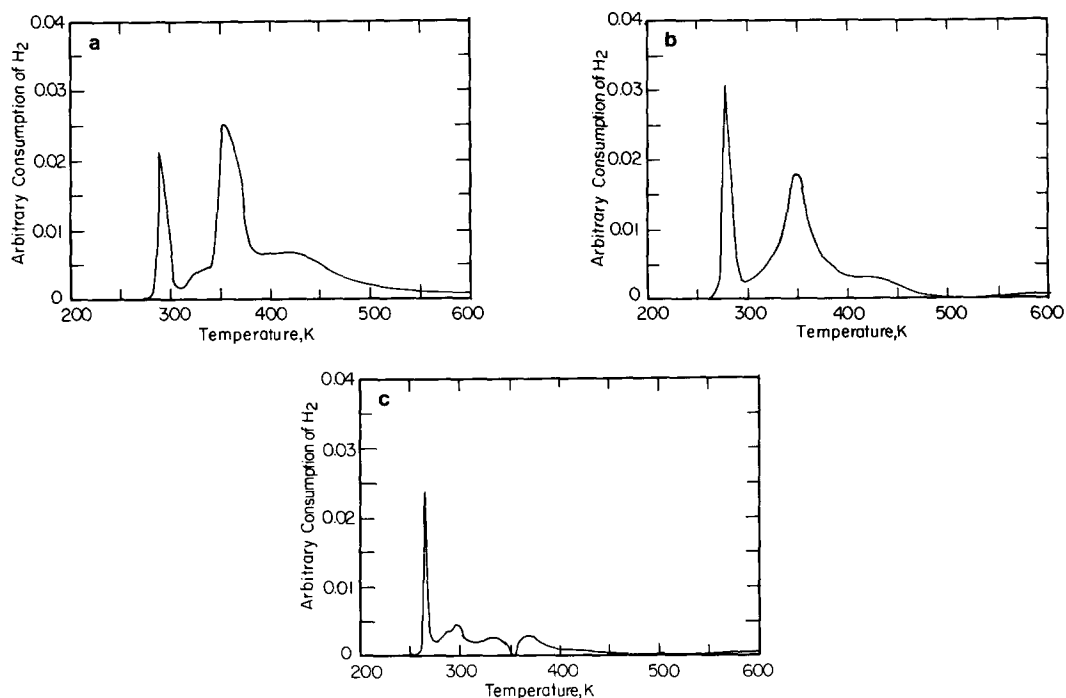


FIG. 4. TPRd profiles of ~3% Pd on: (a) Al₂O₃; (b) 12% WO₃/Al₂O₃; (c) WO₃.

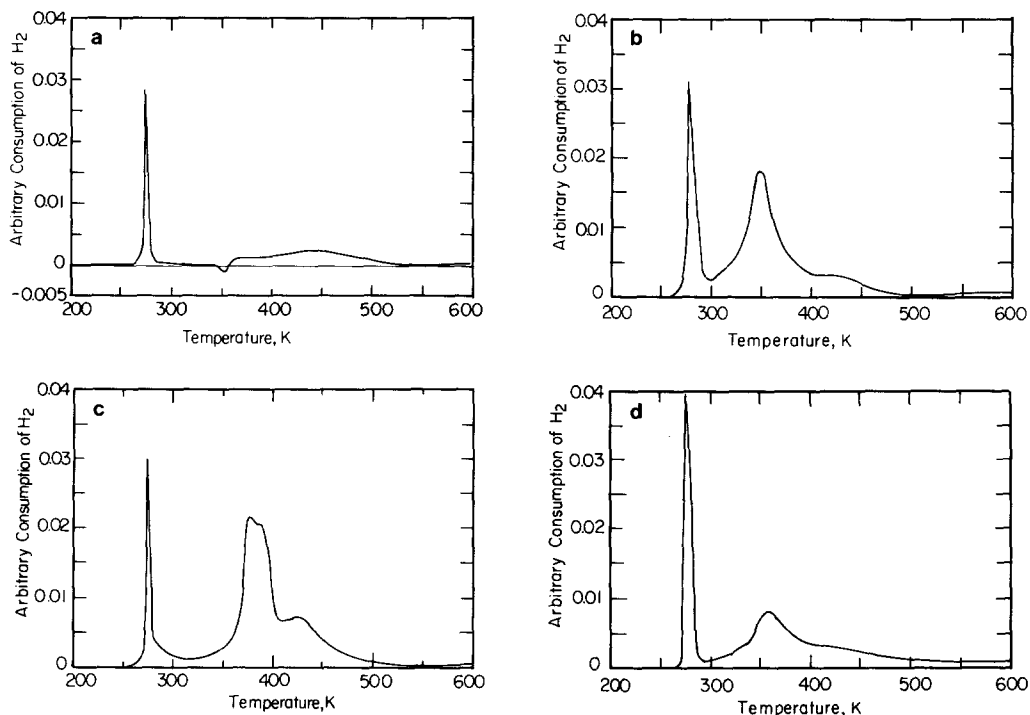


FIG. 5. TPRd profiles of Pd on various composite supports: (a) 1% Pd//12% $\text{WO}_3/\text{Al}_2\text{O}_3$; (b) 3.6% Pd//12% $\text{WO}_3/\text{Al}_2\text{O}_3$; (c) 8.9% Pd//12% $\text{WO}_3/\text{Al}_2\text{O}_3$; (d) 8.9% Pd//30% $\text{WO}_3/\text{Al}_2\text{O}_3$.

ence of WO_3 which is effective in the process. In support of these arguments, Fig. 5 presents additional TPRd profiles for 1.9 and 9% Pd supported on 12% $\text{WO}_3/\text{Al}_2\text{O}_3$ as well as 9% Pd supported on a 30% $\text{WO}_3/\text{Al}_2\text{O}_3$ composite. If Pd^{2+} cations are preferentially adsorbed on the WO_3 portion of the composite due to the presence of favorable electrostatic interaction, then we would expect that over a common support (12% $\text{WO}_3/\text{Al}_2\text{O}_3$) a low loading of Pd might only titrate some of the WO_3 sites, while a higher loading of Pd would not be completely accommodated on the available number of WO_3 adsorption sites. Therefore, a two-peak spectrum would be expected in which the higher temperature peak should be characteristic of $\text{Pd}(\text{NO}_3)_2$. This is clearly what is shown in Figs. 5a and 5b. Furthermore, if at the higher loading of Pd, more WO_3 sites are provided, we would expect that a single peak spectra characteristics of PdO formed by precursor

transformation to oxide on the extra WO_3 sites would result. Figures 5c and 5d provides confirmation of this hypothesis.

TEM

Pd/WO₃. This sample shows phase segregated particles of WO_3 , and Pd and diffraction showed Pd exclusively as PdO. The Pd is located in particles $\approx 0.2 \mu\text{m}$ in diameter. However, these aggregates are porous and contain much smaller crystallites ($\approx 4\text{--}5 \text{ nm}$) of the PdO phase. Thus, the Pd always yields diffraction patterns composed of rings that come from randomly oriented crystallites. On the other hand, though the size of the WO_3 particles is similar, $\approx 0.1\text{--}0.2 \mu\text{m}$, this also is the size of the crystals themselves; hence, the diffraction patterns show spots rather than rings.

Pd/Al₂O₃. The Pd is located in large particles, 40–60 nm in diameter. It is not possible to derive a good average diameter because

TABLE 2
XPS Binding Energies

	Pd 3d _{5/2}	W 4f _{7/2}
3% Pd/Al ₂ O ₃		
Calcined	336.8	
Reduced	335.5	
3.6% Pd/WO ₃ /Al ₂ O ₃		
Calcined	336.9	35.5
Reduced	335.2	35.7
2.5% Pd/WO ₃		
Calcined	336.9	35.5
Reduced	335.3	35.1,33.6
PdO	336.7	

the catalyst is so nonuniform. From EDS, we can tell that all of the Pd is in the dark particles which are readily distinguishable from the alumina support.

Pd//WO₃/Al₂O₃. Here the situation is similar to that on Pd/Al₂O₃ in that all dark identifiable particles on the alumina are Pd particles. However, when EDS was performed from areas that appeared devoid of the large Pd particles, there was still a significant Pd signal. Indeed, closer examination showed smaller Pd particles to be present. The conclusion is that Pd is better dispersed on these samples. However, this has to be moderated by the fact that particles that contained only Pd (no alumina) were also found suggesting that the size distribution may be much broader than that on alumina. Once again, from samples as nonuniform as these, it is impossible to derive particle size averages by a technique such as TEM.

XPS

The Pd 3d_{5/2} and W 4f_{7/2} binding energies for the alumina, composite, and WO₃-supported catalysts are reported in Table 2. The binding energies of Pd in the calcined catalysts were approximately 336.9 eV regardless of the support used. This agrees very well with the binding energy measured for Pd in PdO. When the catalysts are reduced in hydrogen the Pd 3d_{5/2} binding en-

ergy shifts to approximately 335.3 eV, which corresponds to the conversion of PdO to Pd metal. Complete conversion of PdO to metallic Pd was observed for all catalysts.

For the calcined catalysts with tungsten-containing supports, the W 4f_{7/2} binding energy corresponded to the presence of W⁶⁺. Treatment of the composite catalyst in hydrogen resulted in no change in the oxidation state of tungsten. However, reduction of the catalyst supported on WO₃ resulted in the conversion of approximately 36% of the tungsten to a species with a W 4f_{7/2} binding energy of 33.6 eV. The binding energy of this reduced W phase is higher than the value (32.8 eV) previously reported for W⁴⁺ (17), and therefore may correspond to an intermediate W⁵⁺ oxidation state.

Intensity ratios for each of the supported catalysts along with the corresponding average PdO or Pd⁰ particle sizes calculated from those intensity ratios are reported in Table 3. We use the method reported by Stranick *et al.* (18, 19). A general observation is that decreases in Pd 3d/Al 2p and Pd 3d/W 4f intensity ratios are observed upon reduction of each catalyst. This corresponds to an increase in average particle size of the Pd phase when it is converted from the oxide to the metal.

CATALYST PERFORMANCE

The CO TPRx data were used to obtain an estimate of the metal surface areas on each of the supports assuming the number of active sites on each catalyst is based on a 1:1 stoichiometry. We use this method instead of CO chemisorption because metal surface areas and reaction studies can be conveniently obtained on the same sample, *in situ*, and without exposure to the atmosphere after reduction. Figure 6 shows Arrhenius plots of the methanation rate in terms of the TONs for each sample. It is apparent that there is virtually no difference in the activity pattern for the 3% Pd//Al₂O₃ or 3% Pd//12% WO₃/Al₂O₃ catalysts. On the other hand, the 3% Pd/WO₃ has a lower activity than either of these. If a Pd/WO₃

TABLE 3
XPS Data for Pd Catalysts

	I Pd 3d/I Al 2p	I W 4f/I Al 2p	I Pd 3d/I W 4f	Pd size (nm)
3% Pd/Al ₂ O ₃				
Calcined	0.31			2.0
Reduced	0.20			3.0
3.6% Pd/WO ₃ /Al ₂ O ₃				
Calcined	1.60	0.76	2.11	*
Reduced	1.14	0.72	1.58	1.6
2.5% Pd/WO ₃				
Calcined			3.38	2.4
Reduced			1.56	5.3

Note. * = Assumed to be monolayer coverage. Intensity ratios were measured with a precision of $\pm 10\%$ (rsd) or better.

interaction is suppressing the activity of these catalysts and WO₃ centers are favorable adsorption sites during catalyst preparation, then a lower weight loading of Pd on a 12% WO₃/Al₂O₃ catalyst should enable better accommodation of Pd on the WO₃ phase compared to the higher 3% loading of Pd on this support. The activity of a 1% Pd//12% WO₃/Al₂O₃ is also shown in Fig. 6. This catalyst has an activity that is higher than the WO₃ supported Pd but lower than the 3% Pd supported on either Al₂O₃ or the com-

posite. These results are in accordance with the hypothesis presented above.

DISCUSSION

The adsorption-impregnation results shown in Fig. 2 provide strong evidence that the "enhanced" adsorption seen for the 12% WO₃/Al₂O₃ composite compared to Al₂O₃ is due to the presence of WO₃. In conjunction with the cartoon (Fig. 1), those results are interpreted on the basis of a higher population of negative charge carriers on the composite (compared to Al₂O₃), even though the pH of the impregnant was less than the pzc of WO₃. Any further conclusions we reach must be consistent with the fact that as the prevailing conditions during precursor adsorption are such that as the pH decreases from the pH = pH_{pzc} of WO₃, the amount selectively mounted on the second-phase should decrease.

Figures 4 and 5 show the TPRd results from a series of precursors of approximately the same weight loading on each support and the effect of variable weight loading of Pd on composites. We argued earlier that in conjunction with the TPRd signatures of reference compounds that the results shown in Figs. 4 and 5 can be interpreted on the basis that WO₃ acts as a preferred adsorption site in this system. Deconvolution of these spectra, which could not be done be-

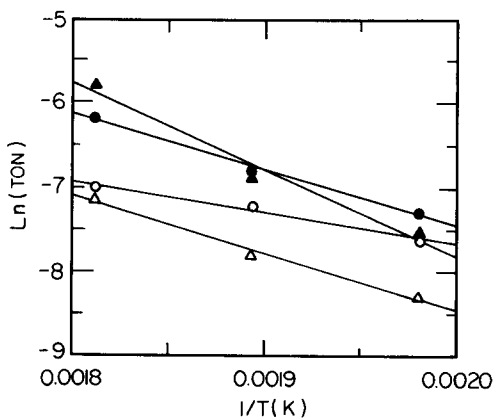


FIG. 6. Methanation activity for each of the catalysts studied. Figure insert denotes catalysts. The composite used (see text) was 12% WO₃/Al₂O₃. Symbols: ▲, 3.3 Pd/Al₂O₃; ●, 3.6 Pd/comp; △, 2.5 Pd/WO₃; ○, 1.9 Pd/comp.

cause of the narrowness of the peaks, was not necessary due to the "sharp" features found for the reference compounds and the catalyst precursors. We now propose that a semiquantitative measure of the degree of partitioning of Pd to the various phases can be obtained by analysis of the results shown in Fig. 4. However, before we do this, some assumptions must be made which appear very reasonable in light of our collective results.

The following assumptions are made:

(1) The TPRd signatures of Pd precursors on the supports correspond to PdO and Pd (precursor)_{ads} where the latter corresponds to the same (chemically) "undissociated" precursor in the adsorbed phase regardless of the support.

(2) The total Pd on any support exists only as PdO and/or Pd (precursor)_{ads}.

(3) The PdO peak height is proportional to its H₂ consumption, and the area of the Pd (precursor)_{ads} signature is proportional to its H₂ consumption.

(4) The speciation of Pd on the supports is: (a) WO₃-PdO; (b) Al₂O₃-PdO and Pd (precursor)_{ads}; (c) composite-PdO and Pd (precursor)_{ads}.

(5) All TPRd data can be normalized to a common weight loading of precursor regardless of the actual weight loading.

With these assumptions and using the weight loadings associated with each support (Fig. 4), the following analysis allows us to estimate the distribution of Pd on the composites.

Let A_C and A_A equal the areas of the peaks corresponding to the Pd (precursor)_{ads} on the composite and alumina, and P_A , P_W , and P_C the heights of the peaks (proportional to area) corresponding to PdO on Al₂O₃, WO₃, and composite. In addition, we introduce a parameter, L_c , to represent the weight percent of Pd on the composite. On the composite, the contribution to P_C comes from both WO₃ and Al₂O₃ phases which we designate as P_{C1} , and P_{C2} , respec-

tively. The "theoretical" peak height for P_C is

$$P_C = P_{C1} + P_{C2} = \left(L_c - \frac{A_C}{(A_A/3.3)} \right) \frac{P_W}{2.5} + \left(\frac{A_C}{(A_A/3.3)} \right) \frac{P_A}{3.3}$$

In this equation, a term such as $A_A/3.3$ corresponds to the area under the reduction profile of a hypothetical 1% Pd//Al₂O₃ catalyst. The bracketed terms are the fraction of Pd on WO₃ and Al₂O₃, respectively, when the total weight loading is L_c . If the assumptions are reasonable, we should be able to compare the "theoretical" value of P_{C1} to that measured experimentally and by assumption (5) also compare the results for 1.9 and 3.6% loadings of Pd on the 12% WO₃/Al₂O₃ composites. The fraction of Pd distributed on each phase, the "theoretical" peak height and the experimental peak heights, P_{C1} , are given in Table 4 along with some additional data discussed below.

The 12% WO₃/Al₂O₃ carrier has ~500 μmol of W. On each of the catalysts (1.9%, 3.6%) 179 and 344 μmol of Pd were available for transfer from the aqueous phase to the carrier. The results presented in Table 4 show that on the 1.9% Pd catalyst virtually all of the Pd is positioned on the WO₃ phase, and proportionally this fraction decreases as the total Pd in the system increases. There is excellent agreement between the theoretical PdO peak height, P_{C1} , and that measured experimentally considering the assumptions we have made.

An explanation for the decrease in Pd partitioning as the Pd content is increased is found if one examines the prevailing pH during preparation. It decreases dramatically as the Pd content in solution increases which is consistent with the fact that Pd(NO₃)₂ is the salt of a very strong acid.

This decrease in pH, we believe, results in two effects. First, as the prevailing pH moves to lower and lower values compared to the pH_{pzc} of WO₃, there are less and less negative charge carriers on this phase,

TABLE 4
Analysis of TPRd Results

Distribution of precursor	$\left\{ \begin{array}{l} \text{on Al}_2\text{O}_3 \text{ (\%)} \\ \text{on WO}_3 \text{ (\%)} \end{array} \right.$	1.9% Pd//	3.6% Pd//
		12% WO ₃ /Al ₂ O ₃	12% WO ₃ /Al ₂ O ₃
		0.064 (6 μmol/g)	2.1 (197 μmol/g)
		1.84 (171 μmol/g)	1.49 (140 μmol/g)
Predicted height of the first peak which corresponds to PdO (P_{Cl})		0.021	0.028
Experimental height of the first peak which corresponds to PdO		0.028	0.030
pH of precursor solution		1.0	0.45

hence adsorption is suppressed. Secondly, WO₃ is "rock stable" at low pH while Al₂O₃ starts to dissolve significantly for pH values <3 (20). We have argued before that this dissolution disrupts the surface of this oxide allowing for some incorporation of Pd²⁺ cations into its structure, thus increasing the partitioning to the Al₂O₃ phase (21). These proposals are entirely consistent with the results reported in Table 4. The results are also consistent with earlier observations we made in a study of Pt//TiO₂/Al₂O₃ (22). Based on experimental results of the dissolution of Al₂O₃, we conclude that it appeared that the presence of a second-phase oxide was instrumental in suppressing acid attack of Al₂O₃. Although we have not conducted such measurements here, we can infer that a similar phenomenon is occurring here. Recall, we reported (Fig. 2) that the buffering action of the supports decreased in the order WO₃ > 12% WO₃/Al₂O₃ > Al₂O₃. If the support is a good buffer, its presence should maintain the pH of the impregnant at its initial value, while for a support which is not a good buffer, the pH will change. An increase in pH in the case of Al₂O₃ initially in contact with electrolytes at low pH is a reflection of Al³⁺ release into the solution and subsequent hydrolysis. This finding implies that *less* Al³⁺ is released in solution for the composite compared to that for Al₂O₃—thus a suppression in dissolution. The possibility of the existence of an "incorporated" Pd in the surface lattice of

Al₂O₃ is discussed later. Now it is useful to turn to the TEM and XPS results.

The TEM results showed effects similar to those we found for Co (1). Specifically, the presence of the second-phase oxide created a different particle size distribution than that formed on Al₂O₃ alone. This finding, again, is consistent with our conclusions that there is a selective metal-support interaction of Pd with the second-phase oxide. The XPS results provide, indirectly, a similar conclusion.

The apparent differences in activity of Pd on the different supports probably do not result from differences in the bulk speciation of Pd based on the results of the XPS analysis. The results show that PdO is probably the exclusive Pd phase on all supports and that when the catalysts are treated in hydrogen the PdO is reduced entirely to metallic Pd on all supports.

The observed differences in activity may be related to differences in the interactions of the PdO and Pd⁰ with the different supports. More specifically, the distribution of the Pd-containing phases between the components of the supports and the dispersion of Pd on the supports may affect activity.

One of the most noticeable results is the large increase in the Pd 3d/Al 2p intensity ratio when Pd is impregnated onto the composite support rather than alumina. Part of the increase can be explained by the larger bulk ratio of Pd to Al in the composite and that the tungsten-containing phase, which is

deposited first, will attenuate some of the signal from the support. However, these two causes alone would only account for a relatively small portion of the overall difference observed in the Pd/Al intensity ratios for the two supports. This leaves an increase in the dispersion of Pd on the composite as the most likely reason for the significant increase in Pd 3d/Al 2p intensity ratios. In fact, the average PdO particle size could not be calculated from the Pd/Al intensity ratio of the calcined composite catalyst because the theoretical value of the Pd/Al intensity ratio calculated for monolayer coverage of Pd (*I*) was less than the measured value. Therefore, it was assumed that the measured Pd 3d/Al 2p intensity ratio corresponds to monolayer coverage of Pd.

The location of a significant amount of Pd on the tungstate phase of the composite support is supported by the XPS results. Specifically, the W 4f/Al 2p intensity ratios for the composite catalysts are approximately one half those reported for a Co//WO₃/Al₂O₃ catalyst, which used the same composite as a support (*I*). The Co on that catalyst had very poor dispersion (average particle size = 200 Å). As seen above, Pd has very good dispersion on the same support. If the Pd were concentrated on the Al₂O₃ alone, then the Al photoelectrons would be attenuated and a higher W/Al intensity ratio would be observed for the catalyst containing Pd. However, if the well-dispersed Pd was covering the tungstate phase, then the W 4f signal would be attenuated and one would indeed observe a lower W/Al intensity ratio, as was seen here. Unlike the Co//WO₃/Al₂O₃ catalyst, the deposition of Pd on the nonreducible tungstate phase in the composite catalyst does not lead to a decrease in the reducibility of Pd.

How the dispersion of Pd affects its activity is not clear. The Al₂O₃ and composite-supported catalysts had the same activity even though the Al₂O₃-supported catalyst had a larger average Pd particle size. Also, the WO₃-supported catalyst, which has the

largest average Pd particle size, showed the lowest activity. Therefore, it appears that some type of synergy between Pd and W and/or Pd and Al₂O₃ is more important than Pd particle size in influencing the activity of the catalyst.

Figure 6 shows that the activity of Pd/Al₂O₃ is approximately an order of magnitude greater than that of Pd/WO₃. Exact comparison is somewhat confounded by the differences seen in apparent activation energy for the reaction. On the 3.3% Pd/Al₂O₃ catalyst tested, there are ~330 μmol Pd/g.cat. Analysis of the TPRd data showed that on a 3.6% Pd//12% WO₃/Al₂O₃ catalyst, ~200 μmol of Pd resided on the Al₂O₃ support. While we treat these values cautiously, they do suggest that the similarity in activity found for 3.3% Pd/Al₂O₃ and 3.6% Pd/composite is simply due to the greater intrinsic activity of Pd supported on Al₂O₃ compared to WO₃.

On the 1.9% Pd/composite, the TPRd results show that a very large fraction of the Pd is partitioned to WO₃ (exact numbers treated cautiously) but some does exist on Al₂O₃. On the basis of the above, we would expect the activity of this catalyst to be greater than Pd/WO₃ due to the "Pd-Al₂O₃" contribution. Indeed, this is what we found.

We cannot rule out other factors such as particle size effects contributing to our findings, but the rationale we have developed seems to point to the conclusion that a major factor controlling the reactivity of this system is due to a selective metal-support exchange.

Finally, we believe it is worthwhile to readdress the possibility of the influence of an incorporated catalytic metal in the support framework due to support dissolution. We distinguish this state from an actual compound (e.g., surface spinel). An indication of this possibility for Ni (23), Ru (24), and Pt (22) has been reported. We have not been successful in providing any direct spectroscopic evidence of this possibility and suggest that others with their arsenal of experi-

mental probes attempt to corroborate their existence.

CONCLUSIONS

There are many reports in the literature that have studied ternary systems of the type described here. Despite the industrial importance of this class of catalysts, there have been few, if any, directed toward a design strategy which could reveal the important preparation parameters that control catalyst performance.

Although it may be premature to put forth generalizations based on only two studies where "design" is correlated with catalyst performance, there are some general conclusions we are positioned to make as a result of our studies of Co//WO₃/Al₂O₃ and Pd//WO₃/Al₂O₃:

(a) A pH-directed selective adsorption onto a specific phase of a composite can be achieved. The "efficiency" of the process appears to improve when the catalytic metal ion complex adsorption is electrostatically controlled.

(b) The pH range over which this phenomenon can occur is not confined to be between the pzc's of the components of the composite oxide. In fact, the range in pH values is also dependent on the ionic strength of the supporting electrolyte because the surface charge depends on this quantity.

(c) If the second-phase oxide is highly dispersed and conditions are such that adsorption is "steered" to that phase, there is a highly dispersed component to the catalytic metal's particle size distribution.

(d) If potential surface compounds have bulk analogs, they likely will be formed during catalyst activation.

(e) The loading level of the active metal precursor can play an important role in catalytic performance due to its partitioning between the components of the composite oxide.

In works currently in progress, we are testing the validity of these assertions and

attempting to establish a scheme whereby new catalyst systems can be proposed based on simple rules.

ACKNOWLEDGMENTS

This work was supported by NSF under Grant CBT-8900514. The electron microscopy was performed at the electron beam microanalysis facility within the Department of Geology at the University of New Mexico. Reference in this report to any specific commercial product, process, or service is to facilitate understanding and does not necessarily imply its endorsement or favoring by the United States Department of Energy. The assistance of J. R. Diehl in the XPS measurements is greatly appreciated.

REFERENCES

1. Zhang, R., Schwarz, J. A., Datye, A., and Baltrus, J. P., *J. Catal.* **135**, 200 (1992).
2. James, R. O., and Park, G. A., *Surf. Colloid. Sci.* **12**, 119 (1982).
3. Fu, L., and Bartholomew, C. H., *J. Catal.* **92**, 376 (1985).
4. Den Hartog, A. J., Deng, M., Jongerius, F., and Ponec, V., *J. Mol. Catal.* **60**, 99 (1990).
5. Contescu, C., and Vass, M. I., *Appl. Catal.* **33**, 759 (1987).
6. Hartley, F. R., "The Chemistry of Platinum and Palladium." Appl. Sci. Publ., London, 1973.
7. Topsøe, H., Clausen, B. S., Topsøe, N. Y., and Pedersen, E., *Ind. Eng. Chem. Fundam.* **25**, 25 (1986).
8. Oh, Se-H., and Eickel, C. C., *J. Catal.* **112**, 543 (1988), and references therein.
9. Hardy, B. E., Baiker, A., Schraml-Marth, M., and Wokaun, A., *J. Catal.* **133**, 1 (1992), and references therein.
10. Brady, R. L., Southmayd, P., Contescu, C., Zhang, R., and Schwarz, J. A., *J. Catal.* **129**, 195 (1991).
11. Huang, Y.-J., Xue, J., and Schwarz, J. A., *J. Catal.* **111**, 59 (1988).
12. Kerkhof, F. P. J. M., and Moulijn, J. A., *J. Phys. Chem.* **83**, 1612 (1979).
13. Huang, Y.-J., Ph.D. dissertation, Syracuse University, Syracuse, New York, 1986.
14. Kester, K. B., Zagil, E., and Falconer, J. K., *Appl. Catal.* **22**, 311 (1986).
15. Sivaraj, Ch., Contescu, Cr., and Schwarz, J. A., *J. Catal.* **132**, 422 (1991).
16. Schwarz, J. A., Ugbor, C. T., and Zhang, R., *J. Catal.* **138**, 38 (1992).
17. Salvati, Jr., L., Makovsky, L. E., Stencel, J. M., Brown, F. R., and Hercules, D. M., *J. Phys. Chem.* **85**, 3700 (1981).
18. Stranick, M. A., Houalla, M., and Hercules, D. M., *J. Catal.* **103**, 151 (1987).

19. Stranick, M. A., Houalla, M., and Hercules, D. M., *J. Catal.* **125**, 214 (1990).
20. Mieth, J. A., Huang, Y.-J., and Schwarz, J. A., *J. Colloid Interface Sci.* **123**, 366 (1988).
21. Mieth, J. A., and Schwarz, J. A., *Appl. Catal.* **55**, 137 (1989).
22. Subramanian, S., and Schwarz, J. A., *Appl. Catal.* **74**, 65 (1991).
23. Huang, Y.-J., Schwarz, J. A., Diehl, J. R., and Baltrus, J. P., *Appl. Catal.* **30**, 163 (1988).
24. Mieth, J. A., and Schwarz, J. A., *J. Catal.* **118**, 203 (1989).